ISSN: 2230-9926

Available online at http://www.journalijdr.com

IJDR

International Journal of Development Research
Vol. 16 Issue, 04, pp. 70322-70331, April, 2026
https://doi.org/10.37118/ijdr.30832.04.2026

RESEARCH ARTICLE OPEN ACCESS

EFFICIENT REMOVAL OF MG DYE FROM TEXTILE EFFLUENT USING MICROWAVE ASSISTED CATALYTIC DEGRADATION BY RICE LIKE MORPHOLOGY MgO/CuO NANOCOMPOSITE

Devi Soundararajan and Rani Thiruvengadam*

Department of Chemistry, Arignar Anna Government Arts College, Villupuram, Affiliated to Thiruvalluvar University, Serkkadu, Vellore – 632 115, Tamil Nadu, India

ARTICLE INFO

Article History:
Received 14th January, 2026
Received in revised form
26th February, 2026
Accepted 08th March, 2026
Published online 30th April, 2026

Key Words:

Malachite Green - MG, Nanocomposite -NC, Gaschromatography-MassSpectrometry - GC-MS, and Microwave Irradiation - MWI.

Corresponding author: Rani Thiruvengadam

ABSTRACT

Continuous release of toxic organic dyes into aquatic environments presents serious environmental and public health concerns, thereby driving the need for effective and sustainable remediation approaches.This studyreports the synthesis of a MgO/CuO nanocomposite (NC) via a facile hydrothermal route and its application as a highly effective catalyst for the degradation of Malachite Green (MG) dye. The structural, morphological, and phase characteristics of the synthesized nanocomposite were comprehensively analyzed using X-ray diffraction (XRD), scanning electron microscopy (SEM), and high-resolution transmission electron microscopy (HR-TEM). XRD analysis confirmed the formation of a heterophase crystalline structure, with an average crystallite size of 17.56 nm calculated using the Debye–Scherrer equation.The catalytic performance of the MgO/CuO nanocomposite was evaluated under microwave irradiation (300 W), achieving a remarkable degradation efficiency of 90.18% within 60 s. The enhanced catalytic activity is attributed to the synergistic interaction between MgO and CuO, which promotes improved charge transfer, increased surface area, and enhanced reactive site availability. The degradation pathway and intermediate species were elucidated using gas chromatography-mass spectrometry (GC-MS, QTOF), providing insights into the underlying reaction mechanism.Furthermore, the effects of key operational parameters, including solution pH, catalyst dosage, and recyclability, were systematically investigated. Notably, high degradation efficiency was achieved even at low catalyst loading, highlighting the material excellent catalytic effectiveness and environmental compatibility. These findings demonstrate that the MgO/CuO nanocomposite is a promising, cost-effective, and eco-friendly candidate for rapid wastewater treatment applications.

Citation: Devi Soundararajan and Rani Thiruvengadam, 2026. "Efficient Removal of mg dye from Textile Effluent using Microwave Assisted Catalytic Degradation by rice like Morphology MgO/CuO Nanocomposite". *International Journal of Development Research*, 16, (04), 70322-70331.

INTRODUCTION

The rapid expansion of the textile industry has led to a substantial increase in the consumption of water and synthetic chemicals, resulting in the large-scale generation of dye-laden wastewater. These effluents contain complex mixtures of organic dyes, auxiliaries, and inorganic salts, many of which are toxic, chemically stable, and resistant to conventional degradation processes [1-4]. To the present knowledge, it is estimated that textile dyeing and finishing processes contribute nearly 20% of global industrial water pollution [5,6]. The presence of dyes in water bodies reduces light penetration, thereby inhibiting photosynthetic activity and decreasing dissolved oxygen levels, which adversely affects aquatic life. Furthermore, many synthetic dyes, particularly azo and triarylmethane dyes, exhibit toxic, mutagenic, and carcinogenic properties [7,8]. Their complex aromatic structures and resistance to biodegradation result in persistent environmental contamination and bioaccumulation in the food chain. Malachite green (MG), a cationic triarylmethane dye, is a representative example of a hazardous organic pollutant frequently detected in industrial effluents. It is widely used in textile dyeing, aquaculture as an antifungal and antiparasitic agent, and as a biological stain [9]. MG is highly soluble in water and exhibits intense coloration due to strong absorption in the visible region (~621 nm). Despite its industrial utility, MG is non-biodegradable and highly persistent, posing significant risks to aquatic organisms and human health. Exposure to MG has been associated with cytotoxicity, genotoxicity, and adverse effects on the liver, kidney, and nervous system [10]. Its stability and widespread use make it a critical target for advanced wastewater treatment technologies.Conventional methods for dye removal, such as coagulation, adsorption, filtration, and biological treatment, often suffer from limitations including incomplete degradation, secondary pollution, and high operational costs [11]. In recent years, nanotechnology has emerged as a powerful approach for environmental remediation, offering innovative solutions for the efficient removal of organic pollutants. Among various nanomaterials, metal oxide nanoparticles (MO-NPs) have attracted considerable attention due to their unique physicochemical properties, including high surface area, tunable electronic structure, and enhanced catalytic activity [12-14].

At the nanoscale, metal oxides exhibit distinct properties compared to their bulk counterparts, primarily due to quantum confinement effects and increased surface reactivity. These features provide a large number of active sites for adsorption and catalytic reactions, making MONPs highly effective for pollutant degradation. In particular, their ability to facilitate electron transfer and generate reactive oxygen species (ROS) under suitable conditions has enabled their widespread application in photocatalysis and advanced oxidation processes [15-17].The performance of metal oxide nanoparticles can be further enhanced through doping or compositing strategies, which modify their structural and electronic properties. Doping with metal or non-metal elements introduces defect states, reduces bandgap energy, and improves charge carrier separation, thereby enhancing catalytic efficiency [18,19]. Transition metals (e.g., Fe, Cu, Mn, Co) and non-metals (e.g., N, C, S) are commonly used dopants to tailor the optical and electronic properties of metal oxides. Such modifications significantly improve visible-light absorption and promote efficient degradation of organic pollutants. Copper oxide (CuO), a p-type semiconductor with a narrow bandgap, has been widely investigated for catalytic and environmental applications. However, its performance can be limited by rapid charge recombination and moderate surface activity. Incorporation of suitable dopants or formation of nanocomposites is an effective strategy to overcome these limitations. Magnesium oxide (MgO), known for its high surface basicity, chemical stability, and non-toxicity, has emerged as a promising component for enhancing the catalytic performance of CuO-based systems. Notably, the similar ionic radii of Mg^{2+} (0.72 Å) and Cu^{2+} (0.73 Å) facilitate effective lattice integration with minimal structural distortion [20].The formation of MgO/CuO nanocomposites can lead to synergistic effects, including improved charge transfer, enhanced surface reactivity, and optimized band structure. These features collectively contribute to superior catalytic performance in pollutant degradation. Moreover, Mg incorporation can modulate the bandgap and improve the generation of reactive species, thereby enhancing the degradation efficiency of persistent organic dyes [21].Various synthesis methods, including sol–gel, co-precipitation, hydrothermal, and microwave-assisted techniques, have been employed to fabricate metal oxide nanostructures with controlled morphology and composition. Among these, the hydrothermal method offers distinct advantages such as uniform particle distribution, high crystallinity, and ease of scalability [22,23]. In this context, the present study focuses on the synthesis of MgO/CuO nanocomposites via a hydrothermal approach and their application in the efficient degradation of malachite green dye. The synergistic interaction between MgO and CuO is expected to enhance catalytic activity through improved surface properties and charge transfer dynamics. This work aims to provide a sustainable and cost-effective solution for the treatment of dye-contaminated wastewater, contributing to the advancement of nanomaterial-based environmental remediation technologies.

EXPERIMENTAL SECTION

MATERIALS

All chemicals were of analytical grade and used as received without further purification. Magnesium sulfate heptahydrate ($MgSO_4 \cdot 7H_2O$, S.D. Fine Chemicals, India), cupric acetate monohydrate ($Cu(CH_3COO)_2 \cdot H_2O$, Qualigens), sodium hydroxide (NaOH, S.D. Fine Chemicals, India), and urea (NH_2CONH_2, S.D. Fine Chemicals, India) were used as precursor materials. Malachite green (MG) dye was obtained from Loba Chemie (India). Deionized (DI) water was used throughout all experimental procedures.

Synthesis of MgO/CuO Nanocomposite: MgO/CuO nanocomposites were synthesized via a hydrothermal method. Initially, typical composition of 3 x 10^{-1} M $Cu(CH_3COO)_2 \cdot H_2O$ and 4.5 x 10^{-3} M $MgSO_4 \cdot 7H_2O$ were dissolved in 50 mL of deionized water under continuous magnetic stirring to form a homogeneous precursor solution. Subsequently, 25 mL of a 2 wt% urea solution was added as a complexing and structure-directing agent.A 10 mL aliquot of 2.5 N NaOH solution was then introduced dropwise into the reaction mixture under vigorous stirring. This step facilitated controlled precipitation, resulting in the formation of a uniform black slurry. The pH of the solution was maintained at ~8 throughout the process to ensure controlled nucleation and growth.Thereafter, 75 mL of the prepared slurry was transferred into a 100 mL Teflon-lined stainless-steel autoclave and subjected to hydrothermal treatment at 160 °C for 24 h. Upon completion, the autoclave was allowed to cool naturally to room temperature.The resulting precipitate was collected, washed repeatedly with deionized water and ethanol to remove residual impurities, and dried at 60 °C for 12 h. Finally, the dried product was calcined at 500 °C for 2 h in a muffle furnace to obtain a highly crystalline MgO/CuO nanocomposite.Using the same synthetic procedure, a series of samples with varying Mg precursor concentrations (4.5 × 10^{-3} to 1.35 × 10^{-2} M $MgSO_4 \cdot 7H_2O$) were prepared and subsequently employed for the degradation of MG dye.In addition, a bulk MgO/CuO sample was synthesized for comparison by dissolving 1.5 M $Cu(CH_3COO)_2 \cdot H_2O$ and 2.25 × 10^{-2} M $MgSO_4 \cdot 7H_2O$ in 50 mL of deionized water, followed by the same preparation procedure described above.

Reaction Mechanism of Nanocomposite Formation: The formation of MgO/CuO nanocomposite involves a sequence of precipitation, hydrothermal transformation, and thermal decomposition processes.Upon addition of NaOH, copper and magnesium ions undergo hydroxide formation:

$$Cu^{2+} + 2OH^- \rightarrow Cu(OH)_2 \downarrow$$

$$Mg^{2+} + 2OH^- \rightarrow Mg(OH)_2 \downarrow$$

Simultaneously, urea undergoes slow hydrolysis under heating conditions, releasing hydroxyl ions that assist homogeneous precipitation:

$$NH_2CONH_2 + 3H_2O \rightarrow 2NH_4^+ + CO_3^{2-} + 2OH^-$$

This controlled release of OH^- ions ensure uniform nucleation and prevents rapid agglomeration of particles.Under hydrothermal conditions (160 °C, 24 h), the initially formed hydroxide precursors undergo dehydration and structural reorganization:

$$Cu(OH)_2 \rightarrow CuO + H_2O$$

$$Mg(OH)_2 \rightarrow MgO + H_2O$$

The elevated temperature and pressure promote crystallization, particle growth, and intimate interfacial contact between MgO and CuO phases.Further thermal treatment at 500 °C enhances crystallinity and phase purity:

$$M(OH)_2 \xrightarrow{\Delta} MO + H_2O (M = Cu, Mg)$$

This step also removes residual organic species and improves structural stability of the nanocomposite.The incorporation of Mg^{2+} ions into the CuO lattice or their coexistence as a secondary MgO phase leads to the formation of a heterostructured nanocomposite. Due to the comparable ionic radii of Mg^{2+} (0.72 Å) and Cu^{2+} (0.73 Å), lattice distortion is minimized, facilitating effective interaction between the two phases. This heterointerface plays a crucial role in enhancing catalytic activity by promoting charge separation and increasing active surface sites.

Characterization: Rigaku D/max-IIIc X-ray diffractometer with Cu kα radiation (λ =0.15406nm,40kv and 45mA) was used to record powder XRD pattern over a 2 theta range from 10º to 80º with step size of 0.02º. The Debye- Scherrer equation was applied to the primary XRD peak for calculating the size of the MgO/CuO nanocomposite.

$$D = \frac{0.89\lambda}{\beta COS\theta}$$

Where D is the crystallite size, λ represents the wavelength of X-ray (λ =0.15406nm), β is the full width at half maximum(FWHM) of the XRD peak in radians, and θ is the diffraction angle in degrees. The surface morphology, elemental composition,crystallitesize and shape, and also crystal structure of the synthesised MgO/CuO nanocomposite particles were analysed using Field Emission Scanning Electron Microscopy(FESEM) equipped with Energy Dispersive X-ray Spectroscopy(EDS) and High-Resolution Transmission Electron Microscopy using a ZEISS-EVO/18 Germany and FEI-TECNAI with model G2-20 TWIN(operating voltage 200kv) respectively. The pathway of toxic dye catalyst assisted degradation was confirmed by Gas chromatography-Mass Spectrometry (GC–MS, QTOF).

Catalytic and Microwave AssistedDegradation Study: In the present study, the catalytic and microwave-assisted degradation of MG dye was systematically investigated using a UV-Visible spectrophotometer (Systronic Model 119). A 10 mL aqueous solution of MG dye with an initial concentration of 10 ppm was used as the standard reaction system for all experiments. To elucidate the individual and combined effects of catalyst and microwave irradiation, three distinct experimental conditions were employed.First, the degradation behavior of MG dye in the absence of catalyst was examined under microwave irradiation at 300 W for 60 seconds, serving as a control to evaluate the sole effect of microwave energy. Second, catalyst-assisted degradation was carried out by introducing 0.01 g of MgO/CuO nanocomposite into the dye solution under ambient conditions, without microwave exposure, to assess the intrinsic catalytic activity. Third, a synergistic approach combining catalyst and microwave irradiation was implemented, wherein the dye solution containing 0.01 g of MgO/CuO nanocomposite was subjected to microwave irradiation at 300 W for varying durations (10, 30, and 60 seconds).

RESULT AND DISCUSSION

X-Ray Diffraction (XRD) Analysis: Figure 1 presents the XRD patterns of MgO/CuO nanocomposite particles synthesized via a hydrothermal route at 160 °C for 24 h, followed by calcination at 500 °C for 2 h. The presence of intense and well-defined diffraction peaks indicates a high degree of crystallinity of the obtained nanocomposite, with no observable secondary or impurity phases. The major diffraction peaks observed at specific 2θ values correspond to the characteristic (11-1), (111), (20-2), (020), (202), and (11-3) planes of monoclinic CuO, (JCPDS No. 01-089-5899) and minor concentration of (01-1), (111), (200), (202), and (301)planes of cubic Cu_2O (JCPDS No. 00-005-0667). In addition, the minor characteristic peaks correspond to crystal planes (111), (200), and (220) planes of the pure hexagonal phase of MgO (JCPDS No. 01- 075-0447). These results confirm the coexistence of both MgO/CuO and Cu_2O phases, indicating the formation of a heterophase copper oxide system (CuO/Cu_2O), but major intense peak revealed the presence of MgO/CuO than the other phase of less percentage Cu_2O phase.The appearance of intense and sharp diffraction peaks reflect the high degree of crystallinity of the synthesized nanocomposite particles. The average crystallite size of the heterophase MgO and CuO nanocomposite particles was estimated using the Debye-Scherrer equation applied to the most intense XRD peak and was found to be approximately 17.56 nm. These findings confirm that the synthesized MgO and CuO nanoparticles are well-crystallized, phase-pure.

Field Emission Scanning Electron Microscopy (FE-SEM) and Energy Dispersive X-Ray Spectroscopy (EDS) Analysis: The surface morphology and microstructural features of the synthesized MgO/CuO nanocomposite particles were examined using Scanning Electron Microscopy (SEM). Figures 2a-e display SEM micrographs of the MgO/CuO samples synthesized via the hydrothermal method at various magnifications.

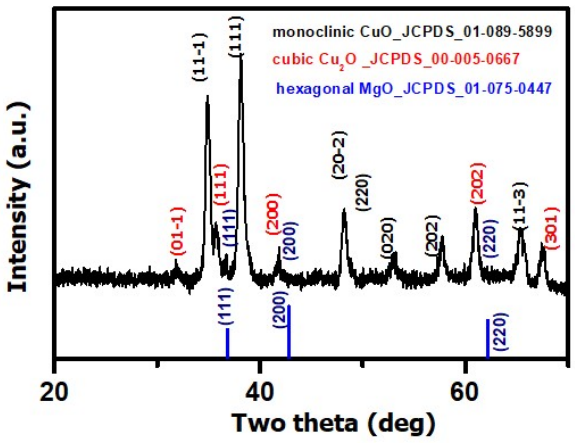

Fig. 1. XRD pattern of MgO/CuO nanocomposite particles synthesized by hydrothermal method at 160ºC for 24 h and heat treated at 500ºC for 2h

The images reveal that the nanoparticles are uniformly distributed with agglomeration as secondary particles. The MgO particles exhibit well-defined fine particles aggregated and distributed over the CuO nanoparticles of high crystalline CuO structures. The average agglomerated particle size was found to be in the range of 300 to500 nm, confirming MgO clusters of nanoparticleswith homogeneous morphology.

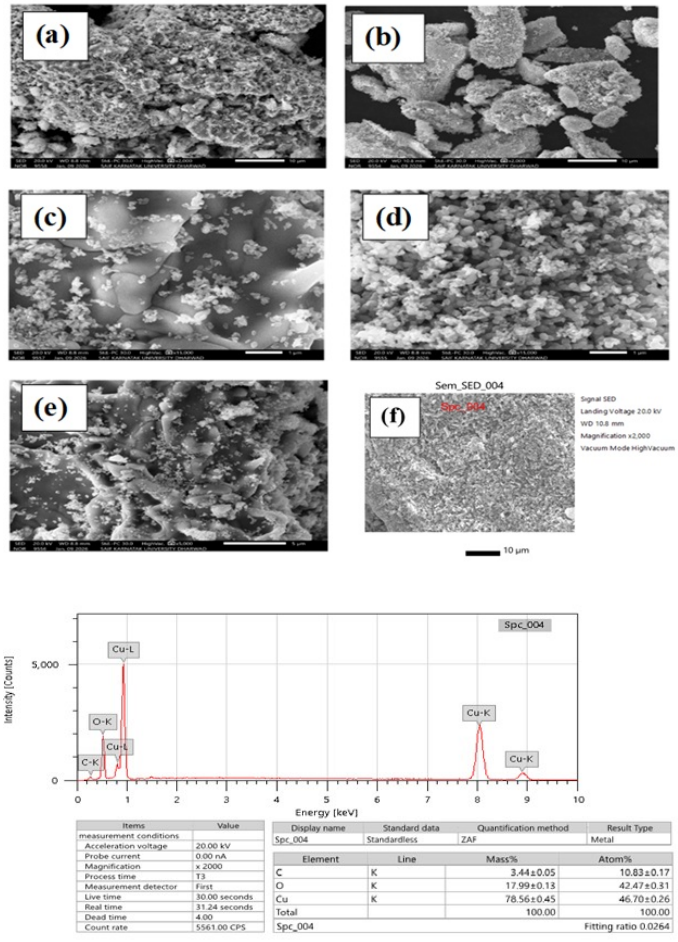

Fig. 2a-e SEM images of catalyst MgO/CuO at different magnifications and (e) EDS Spectrum confirming the elemental composition of Cu and O

Elemental composition analysis was performed using Energy Dispersive X-ray Spectroscopy (EDS), as shown in Fig. 2f. The EDS spectrum exhibited prominent peaks corresponding to copper (Cu) and oxygen (O) at approximately 1keV and 0.5keV, respectively,

confirming the successful formation of copper oxide nanoparticles. The elemental quantification revealed 28.19 wt% of Cu and 25.35 wt% of O, which aligns closely with the theoretical stoichiometric ratio of CuO/Cu_2O. A minor signal of carbon (C) was also detected, likely originating from the use of carbon tape or organic residues from the ethylene glycol precursor.The EDS elemental mapping further verified the uniform distribution of Cu and O throughout the nanoparticle matrix, substantiating the formation of phase-pure copper oxide. In this analysis, as a low concentration of MgO was not been detected, whereas the results verified by the XRD and SEM findings, confirming that the synthesized MgO/CuO nanocomposite particles possess high purity, uniform morphology, and well-defined crystalline structure.

High-Resolution Transmission Electron Microscopy (HRTEM): High-resolution transmission electron microscopy (HRTEM) images (Fig. 3a-f) revealed that the MgO/CuO nanocomposite consists of well-dispersed nanoparticles, indicative of a high surface-to-volume ratio and a large density of accessible active sites. The morphology of the particles exhibits a rice-like structure, with a relatively uniform size distribution characterized by diameters in the range of 50–100 nm and lengths of 150–180 nm. In addition, smaller aggregated clusters with sizes of 5–10 nm are observed, which are attributed to the MgO distributed around CuO phases, respectively.The HRTEM image (Fig. 3g) exhibits clear and well-resolved lattice fringes, demonstrating the high crystallinity of the nanoparticles and enabling direct lattice analysis. The measured interplanar spacings of 0.25 nm and 0.24 nm are indexed to the (111) planes of monoclinic CuO. These values are in good agreement with the XRD results, thereby confirming the crystalline nature and the presence of a MgO/CuO mixed phase in the synthesized material.Furthermore, the selected area electron diffraction (SAED) pattern (Fig. 3h) displays sharp and concentric diffraction rings, further evidencing the high crystallinity and phase purity of the MgO/CuO nanocomposite. The synergistic combination of nanoscale particle dimensions and high crystallinity is anticipated to markedly enhance catalytic performance by facilitating efficient adsorption and promoting effective interfacial interactions with dye molecules.

FT-IR Spectral Analysis: The FT-IR spectrum of the synthesized nanocomposite, recorded in the range of 4000-400 cm^{-1}, is presented in Fig. 4. The broad and intense absorption bands observed in the 3900-3000 cm^{-1} region are attributed to the stretching vibrations of hydroxyl (-OH) groups, indicating the presence of adsorbed water molecules on the nanocomposite surface. Such features also suggest slight surface hydration of the metal oxide nanocomposite upon exposure to ambient atmospheric conditions. Weak absorption bands appearing in the 2400 cm^{-1} region are associated with C-H stretching and bending vibrations. The band observed around 1300 cm^{-1} and a broad and prominent absorption band in the 1100-900 cm^{-1} region is attributed to Cu-O stretching vibrations, confirming the formation of copper oxide within the composite. Furthermore, the absorption features spanning 1100-400 cm^{-1} correspond to the vibrational modes of Mg-O-Cu linkages, providing strong evidence for the successful formation of the MgO/CuO nanocomposite [24]. The existence of robust metal-oxygen interactions within the nanocomposite is further verified by the XRD analysis, indicating structural consistency across characterization techniques.

Effect of Catalytic Activity of MgO/CuO nanocomposite under Microwave Irradiation: Fig. 5 presents the UV-Visible absorbance spectrum of MgO/CuO nanocomposites prepared with varying MgO nanoparticle concentrations (4.5×10^{-3} to 1.35×10^{-2} M), while maintaining a fixed concentration of rice-like structured CuO particles. The degradation efficiency of MG dye was evaluated under MWI at 300 W for 60 s using 0.01 g of the MgO/CuO nanocomposite.As shown in Fig. 5, the nanocomposite with an MgO concentration of 4.5×10^{-3} M exhibited the highest degradation efficiency, achieving approximately 92.91%. Based on this superior performance, the MgO/CuO nanocomposite with 4.5×10^{-3} M MgO was selected for subsequent characterization and further investigations throughout this study.

Effect of Catalytic Activity of MgO/CuO nanocomposite under Microwave Irradiation: Fig.6 illustrates the UV-Visible absorbance spectra for the various concentration of MgO nanoparticles dispersed in a fixed concentration CuO under different experimental conditions:

(a) 10 ppm MG dye solution, (b) MG dye exposed to microwave

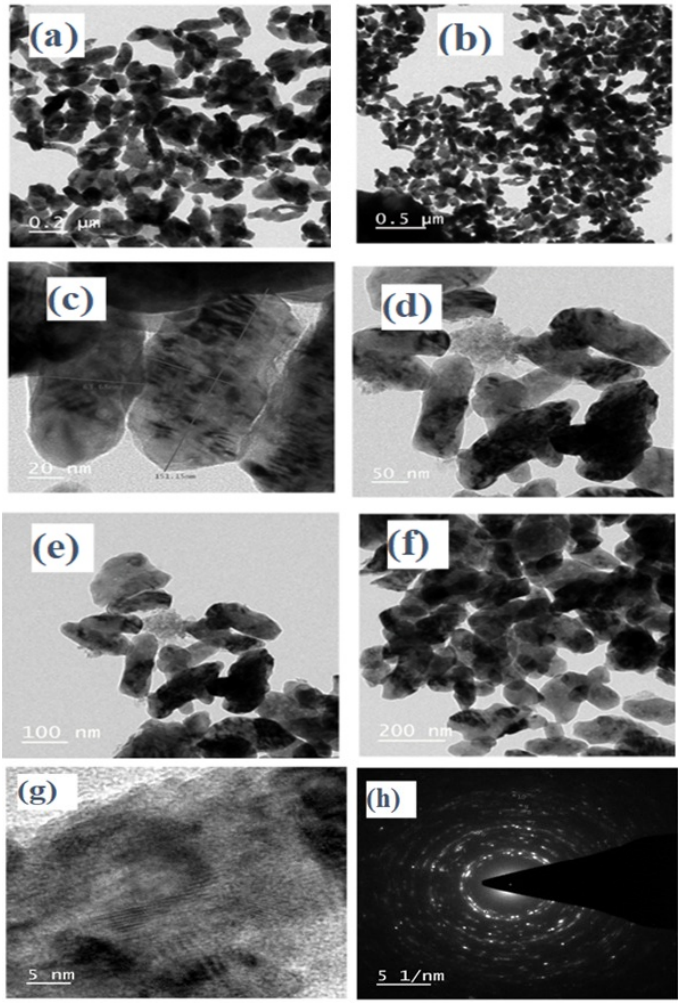

Fig. 3a-f HRTEM images of MgO/CuO nanocomposite g) MgO/CuO at higher magnification and h) SAED pattern for MgO/CuO hydrothermally synthesized at 160ºC for 24 h and heat treated at 500ºC

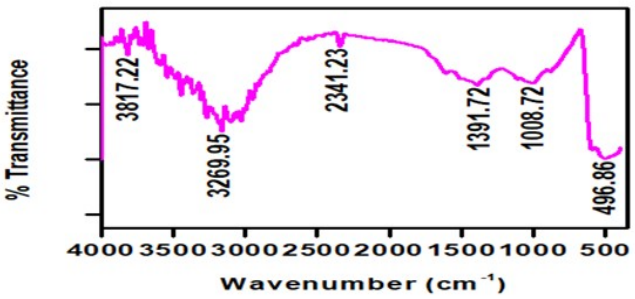

Fig. 4 FT-IR Spectrum of synthesized MgO/CuO nanocomposite

Effect of Catalytic Activity of MgO/CuO nanocomposite under Microwave Irradiation : irradiation(MWI) at 300 W for 60 s, (c) MG dye with 0.01 g MgO/CuOnanocomposite under MWI at 300 W for 60 s at various time intervals, (d) MG dye with 0.01 g MgO/CuO nanocomposite under MWI at 300 W for different irradiation durations, and (e) the corresponding percentage degradation of MG dye under optimized conditions.

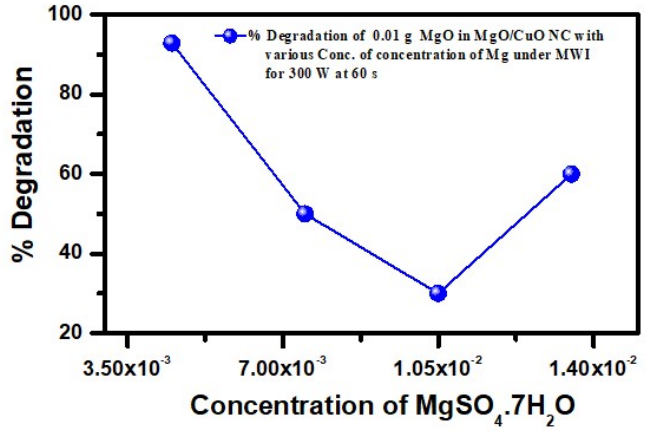

Fig. 5 UV-Visible absorbance spectra for various concentration of $MgSO_4.7H_2O$ in the MgO/CuO nanocomposite and percentage degradation of MG dye with 0.01g MgO/CuO catalyst under microwave irradiation at 300W for 60 s.

The maximum absorbance wavelength (λmax) of MG dye was observed at 616 nm, as shown in Fig. 6a.To elucidate the individual and synergistic effects, experiments were conducted under three conditions, (i) MG dye solution subjected to microwave irradiation at 300 W for 60 s, (ii) MG dye solution containing 0.01 g MgO/CuO nanocomposite under ambient conditions, and (iii) MG dye solution with 0.01 g MgO/CuO nanocomposite under microwave irradiation at 300 W for 10, 30, and 60 s. The temporal variation in absorbance at λ_{max} was monitored, and degradation efficiency was calculated using the relation and is calculated using the equation

$$\% \text{ Degradation} = \frac{C_0 - C_t}{C_0} \times 100$$

where C_0 represents the initial absorbance and Ct denotes the absorbance at time t. The results, along with their graphical representation (Fig. 6), demonstrate a significant enhancement in degradation efficiency (up to 90.18%) under combined catalyst-microwave conditions, highlighting the strong synergistic effect of MgO/CuO nanocomposite and microwave irradiation.

The degradation mechanism, schematically depicted in Fig.7, involves multiple sequential processes, including charge carrier generation, redox reactions, and adsorption-desorption dynamics [25]. Upon microwave irradiation, electrons in the valence band (VB) of the MgO/CuO nanocomposite are excited to the conduction band (CB), leaving behind holes in the VB. These photogenerated electron-hole pairs actively participate in surface redoxreactions. The conduction band electrons reduce dissolved oxygen molecules to form superoxide radicals (O_2^{-}•) [26], while the valence band holes oxidize water molecules to generate hydroxyl radicals (•OH). These highly reactive oxygen species attack the adsorbed MG dye molecules, leading to bond cleavage and progressive degradation.Ultimately, the dye molecules are mineralized into environmentally benign products such as CO_2, H_2O, and simpler non-toxic intermediates. The superior performance of the MgO/CuO nanocomposite under microwave irradiation, compared to individual treatments, confirms its high catalytic efficiency and potential applicability in wastewater remediation.

The overall reaction mechanism can be summarized as:

$$MgO/CuO + h\nu \text{ (microwave)} \rightarrow MgO/CuO\ (e^- + h^+)$$
$$e^- + O_2 \rightarrow O_2^-\bullet$$
$$h^+ + H_2O \rightarrow \bullet OH$$
$$\bullet OH \,/\, O_2^-\bullet + \text{MG dye} \rightarrow \text{Degradation products}$$

A comparative analysis, supported by previously reported studies, was carried out to evaluate the degradation efficiency of the MgO/CuO nanocomposite against various dyes. The results are summarized in Table 1.

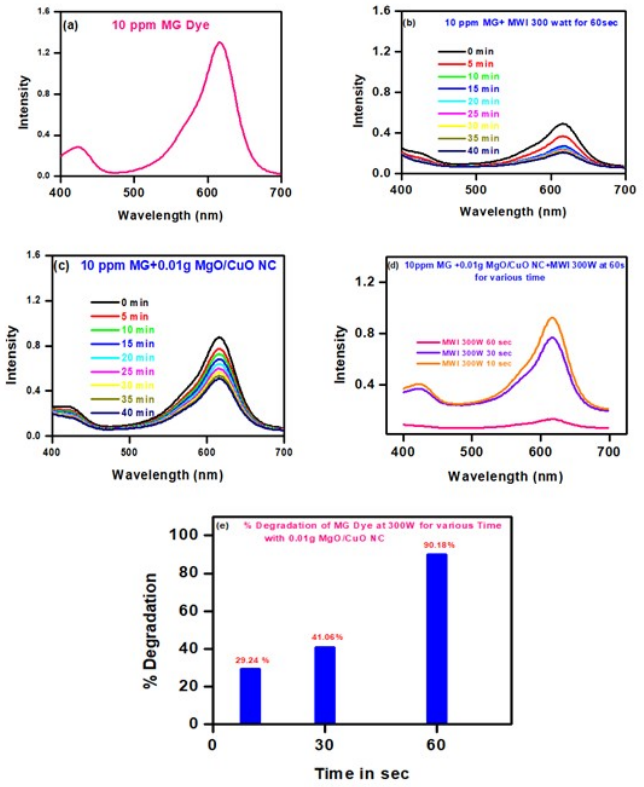

Fig. 6 UV-Visible absorbance spectra for (a)10 ppm MG dye only, (b) MG dye with MWI at 300W for 60 s at various time, (c) 0.01g MgO/CuO catalyst with MG dye under MWI at 300W for 60 s with different time, (d) 0.01g MgO/CuO catalyst with MG dye under MWI at 300W for various seconds and (e) percentage degradation of MG dye with 0.01g MgO/CuO catalyst under microwave irradiation at 300W for 60 s.

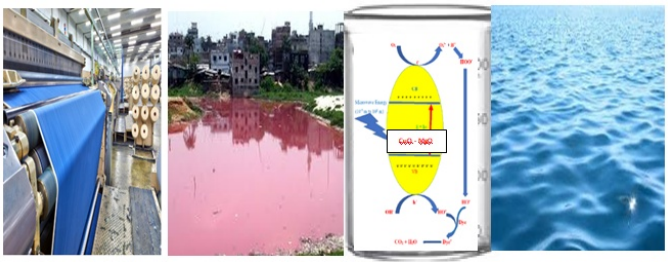

Fig. 7. Schematic representation of the mechanism of dye degradation under MWI at 300w

The data presented in the table clearly indicate that a relatively small amount of MgO/CuO nanocomposite is sufficient to achieve complete degradation of the dye in aqueous media. A key advantage of this approach lies in the ease of recovery and reusability of the synthesized nanocomposite catalyst, highlighting its eco-friendly and cost-effective nature. Photographic evidence of malachite green (MG) dye degradation is shown in Fig. 8, demonstrating that 90.18% degradation was achieved under catalyst-assisted microwave irradiation.The microwave-assisted catalytic degradation significantly reduces reaction time compared to conventional methods and offers a more efficient and selective approach for the removal of toxic dyes from wastewater. This aligns well with the principles of green chemistry by promoting cleaner processing and reduced environmental impact.

Mechanism of MG Dye Degradation via GC–MS (QTOF) Analysis: GC–MS (QTOF) analysis was performed to elucidate the fragmentation pathways of malachite green (MG) dye under microwave-assisted degradation using the MgO/CuO nanocomposite catalyst. The mass spectrum of MG in the presence of 0.01 g catalyst with 10 mL of 10 ppm dye solution is presented in Fig. 9.

Table. 1A comparative study was conducted to assess the degradation efficiency of MgO/CuO nanocomposite with various dyes

S. No	Method	Metal oxide	Particle Size (nm)	Dye	Irradiation	Degradation Efficiency %	Time sec/min/h	Ref.
1	Solgel	MgO/TiO_2	<100	MR	UV light	79.2	60 min	27
2	Solgel	Ag_2S –MgO/GO	29.3	RhB	UV light	98.8	60 min	28
3	Solgel	CuO/MgO	33.5 – 63.2nm.	-	-	-	-	29
4	Solvothermal	CuO/MgO	<100	MO & MB	Visible light	-	-	30
5	Solgel	ZnO/TiO_2	<100	CR	UV light	100	10 min	31
6	Co-precipitation	CuO/MgO	35nm	MB	Visible light	87	60 min	32
7	Co-precipitation	MgO/CuO	19-29 nm	MB	Visible light	-	60 min	33
8	Green Synthesis	CuO/MgO	15.6 nm	MO	Visible light	88.8	NA	34
9	Green Synthesis	MgO/CuO	<100	MB	UV light	89		35
10	Hydrothermal	MgO/CuO	17.56	MG	Microwave Irradiation 300Watt	90.18	60sec	Present work

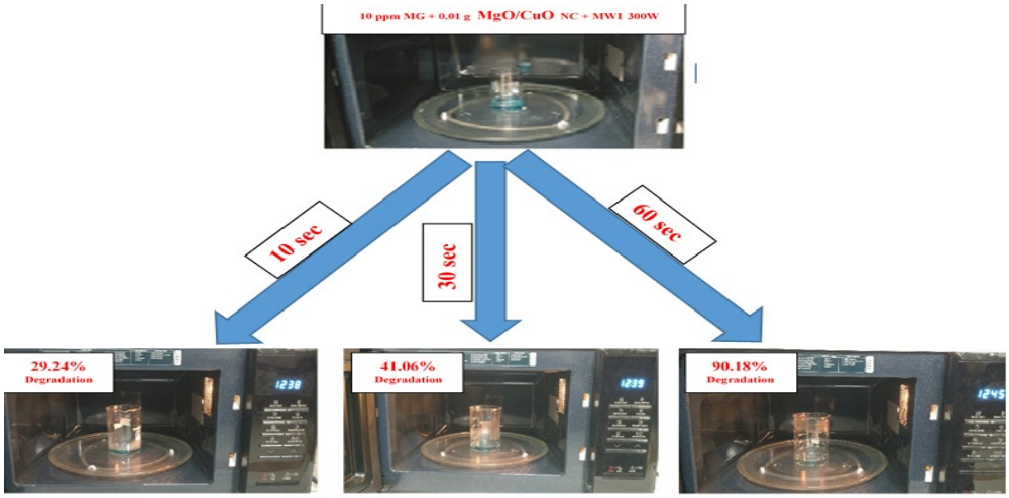

Fig. 8. Photographic image representation of MG dye degradation under MWI

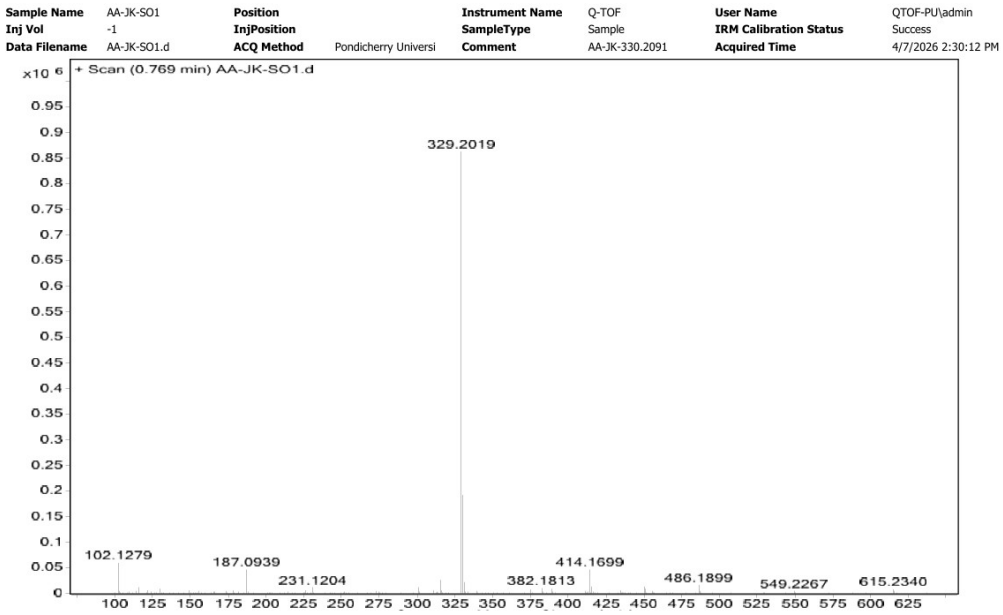

Fig. 9. Mass Spectrum of MgO/CuO nanocomposite(0.01g) with 10mL of 10ppm MG under microwave Irradiation at 300 W for 60s

The proposed mechanism (Fig. 10) shows the molecular ion of MG (m/z =329) undergoes attack by reactive hydroxyl radicals generated due to microwavw-induced electron transitions. This leads to the formation of the intermediate malachite green carbinol (MGC, m/z = 346). In pathway I, this intermediate further fragments into 4-methylaminophenol (4-DMAP, m/z = 137) and 4-dimethylaminobenzophenone (4-DMABP, m/z = 225). Subsequently, 4-DMAP undergoes demethylation to form 4-hydroxyaniline (4-HA, m/z = 109), which is further oxidized into simpler molecules such as CO_2, H_2O, NO_2, and NO.

In parallel, 4-DMABP undergoes demethylation to yield 4-aminobenzophenone (4-ABP, m/z = 197), which is further oxidized to benzaldehyde (BA, m/z = 106) and benzene (B, m/z = 78). In pathway II, the malachite green carbinol intermediate (MGC, m/z = 346) is also cleaved into phenol (P, m/z = 94) and 4,4′-bis(dimethylamino)benzophenone (4,4-BDMABP, m/z = 268). These species undergo subsequent demethylation and hydroxylation, producing less substituted aromatic compounds, which are eventually oxidized to benzaldehyde and benzene.Overall, these degradation routes confirm that the parent dye molecule is progressively broken down into simpler and less harmful products, ultimately completing

the mineralization process into small ionic species such as $C_6H_5^+$, $C_4H_3^+$, and $C_3H_3^+$.

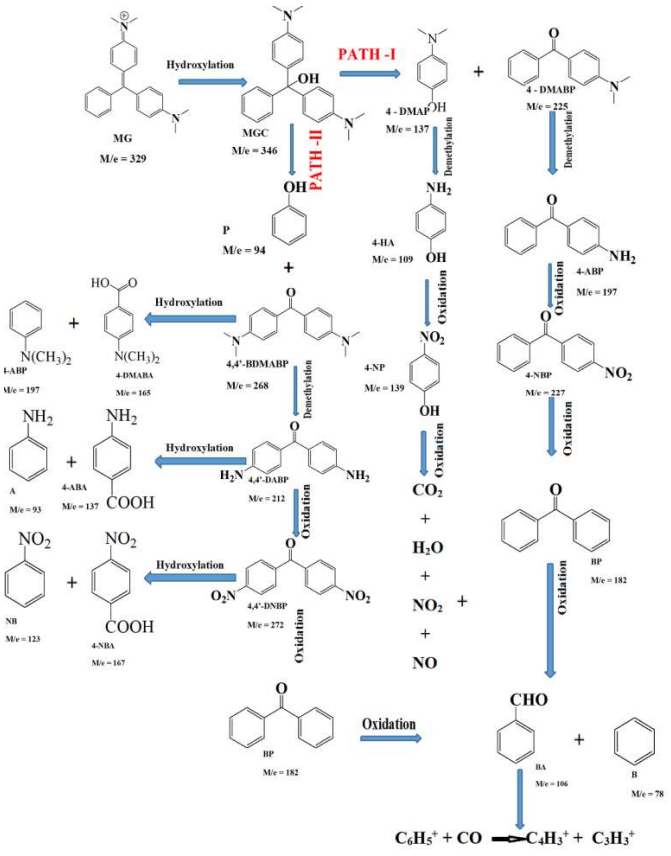

Fig. 10. Breakdown products of MG dye under microwave Irradiation for 300 W at 60 s with MgO/CuO nanocomposite assisted degradation through fragmentation.

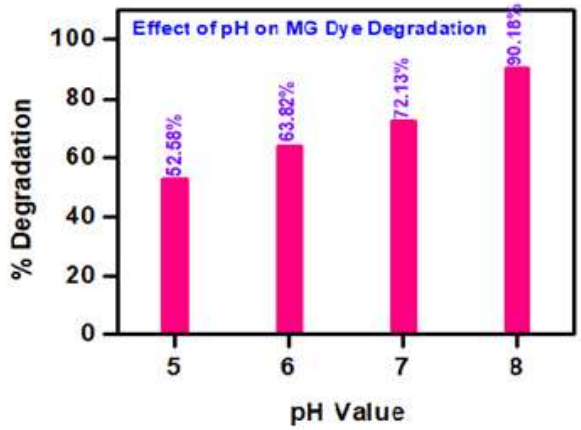

Fig. 11. Effect of pH on % degradation of MG dye under MWI at 60 s

Effect of pH on Dye degradation: Fig. 11, represents the effect of pH on the MG dye degradation using the synthesized MgO/CuO nanomaterials. Recognizing the optimal pH is crucial for enhancing dye degradation efficiency [36]. The surface properties of the synthesized MgO/CuO nanocomposite, as well as the behavior of dissolved dye species, are strongly influenced by the reaction pH [37]. Proper pH optimization also promotes improved adsorption and enhances the generation of reactive species such as hydroxyl (•OH) and hydroperoxyl radicals, along with superoxide anions.The effect of pH in the range of 5-8 on dye degradation was systematically investigated using a catalyst dose of 0.01 g in 10 mL of 10 ppm MG solution under microwave irradiation at 300 W for 60 s. The results showed that degradation efficiency increased with increasing pH, reaching a maximum under basic conditions due to the higher generation of hydroxyl radicals (•OH), which play a dominant role in the oxidation of MG dye. A maximum degradation efficiency of 90.18% was achieved at pH 8, which was identified as the optimum condition, as shown in Fig. 11. Although pH adjustment in wastewater treatment can be time-consuming and costly, it is generally preferable to operate under near-neutral conditions [38]. In the present study, the degradation process was effectively carried out within the pH range of 7-8, ensuring efficient dye removal under near-neutral conditions.

Effect of Catalyst Dosage optimization: The degradation ability of MgO/CuO nanocomposite for the removal of toxic dye was studied by varying the catalyst dosage. The study was conducted by taking variable catalyst dose ranging from0.005 to 0.15g for 10mL of 10ppm MG dye,carried under microwave irradiation at 300W for 60 seconds. The degradation percentage of MG dye was quantitated for each dosage which was shown in Fig. 12. This revealed that the optimal dosage for MgO/CuO catalyst was 0.01g adhering the highest degradation efficacy (90.18%) of MG dye and confirming the effectiveness of the synthesized MgO/CuO catalyst in the rapid degradation of MG dye into harmless CO_2 and H_2O molecules proving the sustainable approach.

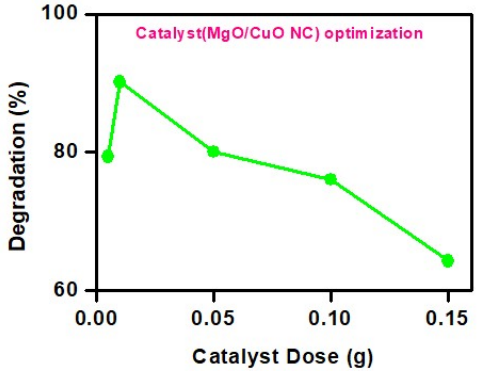

Fig.12 Effect of MgO/CuO catalyst dose for degradation of MG dye

Effectiveness of MgO/CuO nanocomposite compared with bulk MgO/CuO: To confirm the efficacy of the synthesized MgO/CuO nanocomposite, its dye degradation performance was compared with that of the corresponding bulk material prepared via the in-situ doping method, which ensures high homogeneity. The experimental outcomes are presented in Fig. 13a, b, and Fig. 14.The results clearly demonstrate that the nanocomposite exhibits superior degradation efficiency compared to the bulk counterpart.

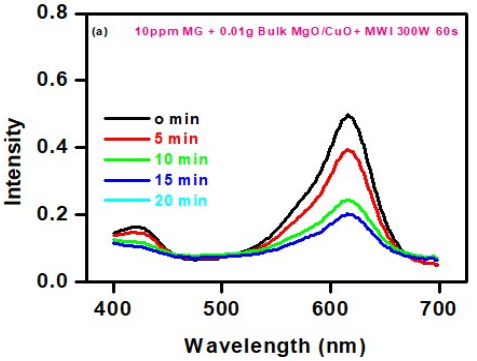

Fig. 13. UV-Visible absorbance spectra of 10 ppm MG dye with MWI 300W at 60 s in the presence of 0.01g of (a) Bulk MgO/CuO (b) NC MgO/CuO

This enhanced performance can be attributed to its higher surface area-to-volume ratio, which provides a greater number of active sites for interaction with malachite green (MG) dye molecules. Consequently, the nanocomposite achieved a degradation efficiency of 90.18%, whereas the bulk material showed only 61.58% under

identical conditions. These findings clearly confirm the high catalytic efficiency of the synthesized MgO/CuO nanocomposite.

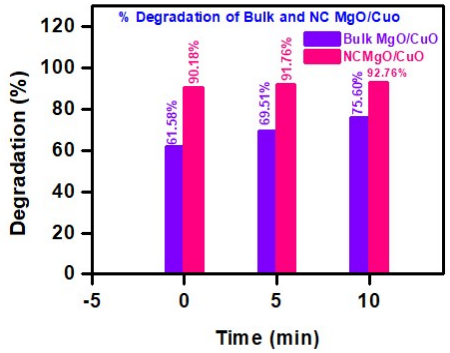

Fig. 14. Bar chart showing the degradation efficiency of 10 ppm MG dye using 0.01 g of bulk and nanocomposite MgO/CuO under microwave irradiation at 300 W for 60 s

Reusability of MgO/CuO nanocomposite: Preventing chemical discharge into landfills helps reduce air, soil, and water contamination while also supporting environmental sustainability through the reuse of materials present in wastewater. Such reuse not only lowers operational costs but also contributes to converting waste into value-added products.With this objective, the reusabilityof the synthesized MgO/CuO nanocomposite for dye degradation was evaluated over five successive cycles, as shown in Fig. 15a andb. After each cycle, the catalyst was recovered by filtration, thoroughly washed with double-distilled water to remove adsorbed dye molecules, and then dried in a hot air oven at 50 °C. Each reuse cycle was conducted under identical optimized conditions for dye degradation.A gradual decrease in degradation efficiency was observed over successive cycles, which may be attributed to minor catalyst loss during handling and recovery.

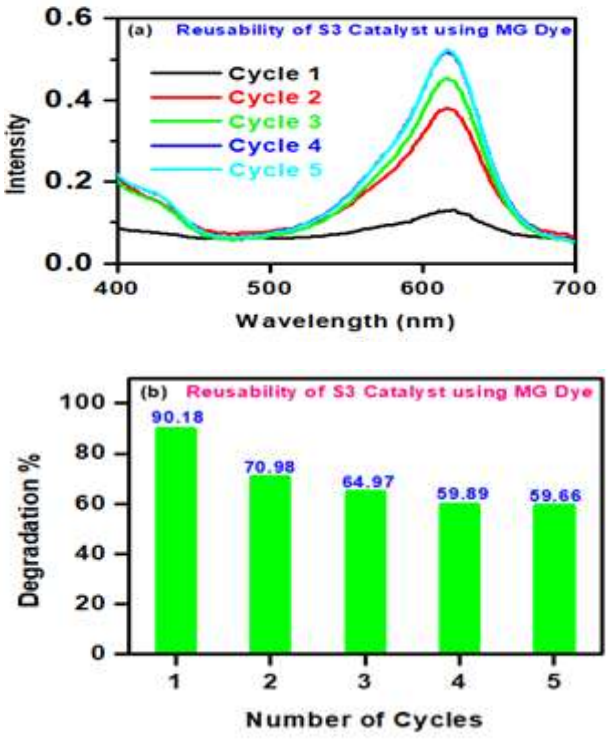

Fig. 15 a) UV-Visible absorbance spectra of MG dye showing reusability of MgO/CuO catalyst and (b) percentage degradation efficiency of MG dye over reuse MgO/CuO catalyst

In addition, accumulation of pollutant species on the active sites likely reduces the availability of reactive centers and limits radical generation, thereby decreasing degradation performance [39]. The degradation efficiencies for malachite green (MG) across five consecutive cycles were 90.18%, 70.98%, 64.97%, 59.89%, and 59.66% at pH 8.Furthermore, increasing the catalyst dosage may help improve both reusability and degradation efficiency. Overall, this study demonstrates a circular economy approach that supports environmental sustainability through catalyst recovery and reuse.

CONCLUSION

The MgO/CuO nanocomposite was successfully synthesized via a hydrothermal process and employed as an efficient catalyst for the degradation of toxic MG dye into less harmful products under microwave irradiation at 300 W for 60 s. The synthesized nanocrystalline nanocomposite exhibited an average crystallite size of 17.56 nm, and its structural, morphological, and compositional characteristics were confirmed through XRD, SEM, HR-TEM, and FT-IR analyses, which collectively revealed its crystallinity, phase composition, and surface morphology.The catalytic performance studies demonstrated that the MgO/CuO nanocomposite achieved a maximum degradation efficiency of 90.18% under optimized conditions. Furthermore, the degradation mechanism was elucidated using GC-MS (QTOF) analysis, confirming the breakdown of MG dye into less toxic intermediates via oxidation, hydroxylation, deamination, and dealkylation pathways under microwave-assisted catalytic conditions. These results strongly support the sustainability of the proposed approach. Overall, the nanocomposite exhibited excellent catalytic efficiency at low dosage and demonstrated good reusability, particularly at pH 8. This study confirms the effectiveness of MgO/CuO nanocomposites as sustainable catalysts for dye degradation and highlights their potential for eco-friendly environmental remediation.

Conflict of Interest: The author hereby declares that there is no conflict of interest.

REFERENCES

1. Samanta, K.K., Pandit, P., Samanta, P. and Basak, S., 2019. Water consumption in textile processing and sustainable approaches for its conservation. In *Water in textiles and fashion* (pp. 41-59). Woodhead Publishing. https://doi.org/10.1016/B978-0-08-102633-5.00003-8
2. Robinson, T., McMullan, G., Marchant, R. and Nigam, P., 2001. Remediation of dyes in textile effluent: a critical review on current treatment technologies with a proposed alternative. *Bioresource technology*, *77*(3), pp.247-255. https://doi.org/10.1016/S0960-8524(00)00080-8
3. Sandin, G. and Peters, G.M., 2018. Environmental impact of textile reuse and recycling–A review. *Journal of cleaner production*, *184*, pp.353-365. https://doi.org/10.1016/j.jclepro.2018.02.266
4. Nigam, P., Armour, G., Banat, I.M., Singh, D. and Marchant, R., 2000. Physical removal of textile dyes from effluents and solid-state fermentation of dye-adsorbed agricultural residues. *Bioresource technology*, *72*(3), pp.219-226. https://doi.org/10.1016/S0960-8524(99)00123-6
5. The Accidental Invention of the Color Mauve Weekly Newsletter,from JSTOR,a non-profit library for the intellectualy curious.
6. Daneshvar, N., Ashassi-Sorkhabi, H. and Tizpar, A., 2003. Decolorization of orange II byelectrocoagulation method. *Separation and purification Technology*, *31*(2), pp.153-162. https://doi.org/10.1016/S1383-5866(02)00178-8
7. Donkadokula, N.Y., Kola, A.K., Naz, I. and Saroj, D., 2020. A review on advanced physico-chemical and biological textile dye wastewater treatment techniques. *Reviews in environmental science and bio/technology*, *19*(3), pp.543-560. https://doi.org/10.1007/s11157-020-09543-z
8. Ahuja, P., Ujjain, S.K., Kanojia, R. and Attri, P., 2021. Transition metal oxides and their composites for photocatalytic dye degradation. *Journal of Composites Science*, *5*(3), p.82. https://doi.org/10.3390/jcs5030082

9. Pereira, A.G., Rodrigues, F.H., Paulino, A.T., Martins, A.F. and Fajardo, A.R., 2021. Recent advances on composite hydrogels designed for the remediation of dye-contaminated water and wastewater: A review. *Journal of Cleaner Production*, *284*, p.124703. https://doi.org/10.1016/j.jclepro.2020.124703
10. Kishor, R., Purchase, D., Saratale, G.D., Saratale, R.G., Ferreira, L.F.R., Bilal, M., Chandra, R. and Bharagava, R.N., 2021. Ecotoxicological and health concerns of persistent coloring pollutants of textile industry wastewater and treatment approaches for environmental safety, *Journal of Environmental Chemical Engineering*, *9*(2), p.105012. https://doi.org/10.1016/j.jece. 2020.105012.
11. Sen, S., Das, C., Ghosh, N.N., Baildya, N., Bhattacharya, S., Khan, M.A., Sillanpää, M. and Biswas, G., 2022. Is degradation of dyes even possible without using photocatalysts?–a detailed comparative study. *RSC advances*, *12*(53),pp.34335-34345. https://doi.org/10.1039/D2RA05779D
12. Kadirvelu, K., Kavipriya, M., Karthika, C., Radhika, M., Vennilamani, N. and Pattabhi, S., 2003. Utilization of various agricultural wastes for activated carbon preparation and application for the removal of dyes and metal ions from aqueous solutions. *Bioresource technology*, *87*(1), pp.129-132. https://doi.org/10.1016/S0960-8524(02)00201-8
13. Lee, K.M., Lai, C.W., Ngai, K.S. and Juan, J.C., 2016. Recent developments of zinc oxide based photocatalyst in water treatment technology: a review. *Water research*, *88*, pp.428-448.https://doi.org/10.1016/j.watres.2015.09.045
14. Fabrega, J., Luoma, S.N., Tyler, C.R., Galloway, T.S. and Lead, J.R., 2011. Silver nanoparticles: behaviour and effects in the aquatic environment. *Environment international*, *37*(2), pp.517-531.https://doi.org/10.1016/j.envint.2010.10.012
15. Rassaei, L., Marken, F., Sillanpää, M., Amiri, M., Cirtiu, C.M. and Sillanpää, M., 2011. Nanoparticles in electrochemical sensors for environmental monitoring. *TrAC Trends in Analytical Chemistry*, *30*(11), pp.1704-1715. https://doi.org/10.1016/ j.trac.2011.05.009
16. Marimuthu, S., Antonisamy, A.J., Malayandi, S., Rajendran, K., Tsai, P.C., Pugazhendhi, A. and Ponnusamy, V.K., 2020. Silver nanoparticles in dye effluent treatment: A review on synthesis, treatment methods, mechanisms, photocatalytic degradation, toxic effects and mitigation of toxicity. *Journal of Photochemistry and Photobiology B: Biology*, *205*, p.111823. https://doi.org/10.1016/ j.jphotobiol.2020.111823
17. Ahmed, T., Noman, M., Shahid, M., Niazi, M.B.K., Hussain, S., Manzoor, N., Wang, X. and Li, B., 2020. Green synthesis of silver nanoparticles transformed synthetic textile dye into less toxic intermediate molecules through LC-MS analysis and treated the actual wastewater. *Environmental Research*,*191*, p.110142. https://doi.org/10.1016/j.envres.2020.110142
18. Fang, Z., Qiu, X., Chen, J. and Qiu, X., 2011. Debromination of polybrominated diphenyl ethers by Ni/Fe bimetallic nanoparticles: influencing factors, kinetics, and mechanism. *Journal of Hazardous Materials*, *185*(2-3), pp.958-969. https://doi.org/10.1016/j.jhazmat.2010.09.113
19. Siripireddy, B. and Mandal, B.K., 2017. Facile green synthesis of zinc oxide nanoparticles by Eucalyptus globulus and their photocatalytic and antioxidant activity. *Advanced Powder Technology*, *28*(3), pp.785-797. https://doi.org/10.1016/ j.apt.2016.11.026
20. da Silva, A.F.V., Fagundes, A.P., Macuvele, D.L.P., de Carvalho, E.F.U., Durazzo, M., Padoin, N., Soares, C. and Riella, H.G., 2019. Green synthesis of zirconia nanoparticles based on Euclea natalensis plant extract: Optimization of reaction conditions and evaluation of adsorptive properties. *Colloids and Surfaces A: Physicochemical and Engineering Aspects*, *583*, p.123915. https://doi.org/10.1016/j.colsurfa.2019.123915
21. Sharaf El-Deen, S.E.A. and Zhang, F.S., 2016. Immobilisation of TiO2-nanoparticles on sewage sludge and their adsorption for cadmium removal from aqueous solutions. *Journal of experimental nanoscience*, *11*(4), pp.239-258. https://doi.org/ 10.1080/17458080.2015.1047419
22. Sharmin, M., Esha, I.N., Begum, T., Rahman, A. and Maria, K.H., 2025. Influence of Mg doping on Growth, Structural, Morphological, Optical, and Electrical Properties of CuO Thin Films: Experimental and DFT studies. *Micro and Nanostructures*, p.208486.https://doi.org/10.1016/j.micrna.2025.208486
23. Babu, M.M.H., Podder, J., Tofa, R.R. and Ali, L., 2021. Effect of Co doping in tailoring the crystallite size, surface morphology and optical band gap of CuO thin films prepared via thermal spray pyrolysis. *Surfaces and Interfaces*, *25*, p.101269. https://doi.org/ 10.1016/j.surfin.2021.101269
24. Ramimoghadam, D., Bagheri, S. and Abd Hamid, S.B., 2014. Biotemplated synthesis of anatase titanium dioxide nanoparticles via lignocellulosic waste material. *BioMed research international*, *2014*(1), p.205636. https://doi.org/10.1155/ 2014/205636
25. Elkady, M.F. and Hassan, H.S., 2021. Photocatalytic degradation of malachite green dye from aqueous solution using environmentally compatible Ag/ZnO polymeric nanofibers. *Polymers*, *13*(13), p.2033.https://doi.org/10.3390/polym13132033
26. Ye, L., Chen, J., Tian, L., Liu, J., Peng, T., Deng, K. and Zan, L., 2013. BiOI thin film via chemical vapor transport: photocatalytic activity, durability, selectivity and mechanism. *Applied Catalysis B: Environmental*, *130*, pp.1-7. https://doi.org/10.1016/j.apcatb. 2012.10.011
27. Zahra, S., Mazhar, S., Zahra, S., Idrees, H. and Hussnain, A., 2022. Synthesis and characterization of magnesium doped titania for photocatalytic degradation of methyl red. *Matéria (Rio de Janeiro)*, *27*, p.e13160. https://doi.org/10.1590/S1517-707620220001.1360
28. Wang, H., Li, G., & Fakhri, A. (2020). Fabrication and structural of the Ag2S-MgO/graphene oxide nanocomposites with high photocatalysis and antimicrobial activities. Journal of Photochemistry and Photobiology B: Biology, 207, 111882. https://doi.org/10.1016/j.jphotobiol.2020.111882
29. Yassen, D.A., Othman, F.M. and Hamead, A.A., 2021, February. Preparation and Characterization of CuO/MgO Nano Particles using Sol-Gel Technique. In *IOP Conference Series: Materials Science and Engineering* (Vol. 1094, No. 1, p. 012163). IOP Publishing. doi:10.1088/1757-899X/1094/1/012163.
30. Alla, S.K., Verma, A.D., Kumar, V., Mandal, R.K., Sinha, I. and Prasad, N.K., 2016. Solvothermal synthesis of CuO–MgO nanocomposite particles and their catalytic applications. *RSC advances*, *6*(66), pp.61927-61933. DOI: 10.1039/c6ra03762c.
31. Janitabar-Darzi, S. and Mahjoub, A.R., 2009. Investigation of phase transformations and photocatalytic properties of sol–gel prepared nanostructured ZnO/TiO2 composites. *Journal of Alloys and Compounds*, *486*(1-2), pp.805-808. doi:10.1016/ j.jallcom.2009.07.071.
32. Pricilla, R.B., Elsie, A.S., Mohan, A., Kumar, V.M., Vidhya, B. and Nandhakumar, R., 2021. Studies on the structural, optical and photocatalytic properties of CuO/MgO nanocomposite prepared by facile chemical co-precipitation. *Materials Today: Proceedings*, *47*, pp.837-842. https://doi.org/10.1016/ j.matpr.2020.12.791
33. Jeetendra Kulkarni, R. Ravishankar, H. Nagabhushana, K.S. Anan tharaju, R.B. Basavaraj, M. Sangeeta, H.P. Nagaswarupa, L.Renu ka., 2017. *MaterialsToday: Proceedings*, 11, pp.11756-11763. https://doi.org/10.1016/j.matpr.2017.09.092.
34. Abbas, S., Uzair, B., Sajjad, S., Leghari, S.A.K., Noor, S., Niazi, M.B.K., Farooq, I. and Iqbal, H., 2022. Dual-functional green facile CuO/MgO nanosheets composite as an efficient antimicrobial agent and photocatalyst. *Arabian Journal for Science and Engineering*, *47*(5), pp.5895-5909. https://doi.org/ 10.1007/s13369-021-05741-1.
35. Priya, R., Stanly, S., Dhanalekshmi, S.B. and Sagadevan, S., 2019. Fabrication of photocatalyst MgO: CuO composite and enhancement of photocatalytic activity under UV light. *Materials Research Express*, *6*(12), p.125023. DOI 10.1088/2053-1591/ab53f6
36. Soundararajan, D., Pandurangan, M. and Thiruvengadam, R., 2025. Ultra fast microwave irradiation based catalytic degradation of dyes by magnesium oxide nanoparticles. *Journal of Water and*

Environmental Nanotechnology, *10*(1), pp.8-23. https://doi.org/10.22090/jwent.2025.01.02

37. Gurusamy Thangam, P., Pattulingam, R., Vellaiyan, V., Murugaesan, B. and Sathasivam, K., 2024. Enhanced Photocatalytic Degradation of methylene blue dye using Co3O4 nanoparticles from the fruit extracts of diplocyclos Palmatus (L) C. Jeffrey for wastewater remediation. *Journal of Water and Environmental Nanotechnology*, *9*(3), pp.356-366. https://doi.org/10.22090/jwent.2024.03.08
38. Mohamed, A., Mahanna, H. and Samy, M., 2024. Synergistic effects of photocatalysis-periodate activation system for the degradation of emerging pollutants using GO/MgO nanohybrid. *Journal of Environmental Chemical Engineering*, *12*(2), p.112248. https://doi.org/10.1016/j.jece.2024.112248
39. Deng, H., 2020. Ozonation mechanism of carbamazepine and ketoprofen in RO concentrate from municipal wastewater treatment: Kinetic regimes, removal efficiency and matrix effect. *Science of The Total Environment*, *717*, p.137150. https://doi.org/10.1016/j.scitotenv.2020.137150

****